Dynamic conformal arc cranial stereotactic radiosurgery: implications of multileaf collimator margin on dose–volume metrics

[1,2]J A TANYI, PhD, [3]E J DOSS, MD, [4]C M KATO, [1]D L MONACO, RT(R)(T), CMD, [1]L Z MENG, PhD, [5]Y CHEN, PhD, [1]C D KUBICKY, MD, PhD, [1]C M MARQUEZ, MD and [1,2]M FUSS, MD, PhD

[1]*Department of Radiation Medicine, Oregon Health and Science University, Portland, OR, USA,* [2]*Department of Nuclear Engineering and Radiation Health Physics, Oregon State University, Corvallis, OR, USA,* [3]*Department of Internal Medicine, Providence St. Vincent Medical Center, Portland, OR, USA,* [4]*Macalester College, Saint Paul, MN, USA, and* [5]*Department of Public Health & Preventive Medicine, Oregon Health and Science University, Portland, OR, USA*

Objective: The effect of multileaf collimator (MLC) margin on target and normal tissue dose–volume metrics for intracranial stereotactic radiosurgery (SRS) was assessed.
Methods: 118 intracranial lesions of 83 SRS patients formed the basis of this study. For each planning target volume (PTV), five separate treatment plans were generated with MLC margins of −1, 0, 1, 2 and 3 mm, respectively. Identical treatment planning parameters were employed with a median of five dynamic conformal arcs using the Varian/BrainLab high-definition MLC for beam shaping. Prescription dose (PD) was such that 22 Gy covered at least 95% of the PTV. Dose–volume and dose–response comparative metrics included conformity index, heterogeneity index, dose gradient, tumour control probability (TCP) and normal tissue complication probability (NTCP).
Results: Target dose heterogeneity decreased with increasing MLC margin ($p<0.001$); mean heterogeneity index decreased from 70.4 ± 12.7 to $10.4\pm2.2\%$. TCP decreased with increasing MLC margin ($p<0.001$); mean TCP decreased from 81.0 ± 2.3 to $62.2\pm1.8\%$. Normal tissue dose fall-off increased with MLC margin ($p<0.001$); mean gradient increased from 3.1 ± 0.9 mm to 5.3 ± 0.7 mm. NTCP was optimal at 1 mm MLC margin. No unambiguous correlation was observed between NTCP and PTV volume. Plan delivery efficiency generally improved with larger margins ($p<0.001$); mean monitor unit per centigray of the PD decreased from 3.60 ± 1.30 to 1.56 ± 0.13.
Conclusion: Use of 1 mm MLC margins for dynamic conformal arc-based cranial radiosurgery resulted in optimal tumour control and normal tissue sparing. Clinical significance of these comparative findings warrants further investigation.

Stereotactic radiosurgery (SRS) is characterised by focal ablative doses to small discrete target volumes (<35 cm^3), steep dose gradients, and precise and reliable targeting, in order to minimise untoward effects on normal and/or critical structures, while simultaneously optimising target doses. Accordingly, a high degree of conformality or conformal planning is a fundamental principle of SRS, defined by the precise matching of the discrete target volume being irradiated with the target pathology. SRS has an entrenched role in the treatment of benign and malignant neurological indications. In recent years, linear accelerator (linac)-based SRS has gained increased relevance in the management of cranial presentations (*e.g.* brain metastases) and has become a customary treatment modality. Historically, linac-based SRS treatment planning and delivery has relied upon multiple intersecting non-coplanar arcs and small (≤40 mm) circular collimators, capable of producing steep-gradient, spherical dose distributions similar to those generated by the Gamma Knife technique [1–2]. However, over the last 15 years, multileaf collimators (MLCs), now routine appendages to modern linacs and major field-shaping devices in radiotherapy, have evolved in terms of both field size and individual tungsten leaf width, and have facilitated various methods for physical SRS dose delivery, including three-dimensional conformal beams, intensity-modulated beams and dynamic conformal arcs (DCAs). To closely approximate the smooth edge of custom shielding blocks, finer-resolution MLC leaves are, in theory, required [3]. Nonetheless, MLCs provide, to some extent, a slightly wider physical beam penumbra than custom shielding blocks [4–5]. Hence, an additional margin around the planning target volume may be necessary to account for penumbra effects. Cardinale et al [6] and Jin et al [7] have performed systematic assessments

investigating the optimal beam margins in extracranial stereotactic radiotherapy. However, interpretation of true dose–response relationships is an intricate process due to variations in radiosurgery planning practices between institutions, as well as potential interpatient variability within institutions. The current study assesses the dosimetric implications of physical beam penumbra compensation with varying MLC blocking margins around the planning target volume on clinically generated SRS treatment plans.

Methods and materials

Patient population

The current retrospective analysis was approved by our institutional review board, with patient informed consent waiver. Medical records of patients who underwent stereotactic radiosurgery (SRS) for cranial presentations at our institution between June 2008 and August 2010 were reviewed for this study. 118 spherical or quasi-spherical metastatic brain lesions of 86 patients formed the basis of the current comparative analysis.

Treatment planning

High-resolution (1 mm slice thickness) CT scans (Philips Medical Systems, Cleveland, OH) were used for treatment planning on a dedicated radiotherapy planning platform (iPlan RT Dose 4.1.0; BrainLAB AG, Heimstetten, Germany). Radiosurgery plans were based on five default DCAs spread evenly over a 2π steradian solid angle, with practical modification of number of arcs and/or arc length and/or couch angle according to tumour and critical organ location. Beam shaping utilised a high-resolution MLC system (HD-MLC; 2.5 mm at isocenter; Novalis Tx, BrainLAB). Five separate plans with identical dose calculation parameters except for the MLC margin were generated for each planning target volume (PTV). For the purpose of the current study, the PTV was a zero-margin-expansion of the gross tumour volume. Corresponding MLC margins were −1, 0, 1, 2 and 3 mm. To circumvent any dose interference resulting from simultaneous treatment of multiple targets, all cases were planned as having a single lesion. Dose computation was based on a pencil beam algorithm for 6 MV photon beam energy at a maximum dose rate of 1000 monitor units per minute (MU min^{-1}). Tissue heterogeneity was taken into account. An adaptive dose matrix with an upper limit of 2 mm was used for dose–volume computation; this allowed for automatic adjustment of dose resolution such that a minimum of 10 voxels were always used for dose computation on each dimension inside a target volume of interest, irrespective of the latter's geometry. Plan normalisation was such that a prescription dose (PD) of 22 Gy encompassed at least 95% of the PTV. It should be emphasised that while individual clinical prescription doses were based on factors including tumour size, location and proximity to critical structures, as well as patient performance status, a PD of 22 Gy was used for the purpose of this study to ensure standardised and unbiased comparison. 590 treatment plans comprised the current analysis.

Evaluation parameters

Target volumes were categorised as follows: PTV < 1 cm^3 (''small lesions''; $n = 65$), $1 \leq$ PTV <5 cm^3 (''medium lesions''; $n = 41$) and PTV ≥ 5 cm^3 (''large lesions''; $n = 12$). A peritumoral rind volume, defined in the current study as a 20-mm wall from the surface of the PTV, was used to characterise normal tissue. The following dose–volume comparative metrics were computed for corresponding plan evaluation. A heterogeneity index (HI) was mathematically defined as [8]:

$$HI = \frac{D_{max} - D_{min}}{D_{mean}} \qquad (1)$$

where D_{mean} is defined in this study as the sum of the product of dose value and percentage volume in each dose bin, D_{min} as the dose to 99% of the PTV, and D_{max} as the dose received by the ''hottest'' 3% volume of the PTVs that were computed and recorded. A conformity index (CI) was mathematically defined as [9–10]:

$$CI = \frac{V_{PTV} \times V_{PIS}}{[PTV_{PIS}]^2} \qquad (2)$$

where PIS is the prescription isodose surface, V_{PTV} is the magnitude of the planning target volume, V_{PIS} is the volume encompassed by the prescription isodose surface, and PTV_{PIS} is the planning target volume encompassed within the prescription isodose surface. A gradient score index (distance in mm) [11] was defined mathematically as

$$G = 100 \times [1 - [(R_{eff,Rx} - R_{eff,50\%Rx}) - 0.3]] \qquad (3)$$

where $R_{eff,Rx}$ is the effective radius of the prescription isodose volume and $R_{eff,50\%Rx}$ is the effective radius of the isodose line equal to one-half of the prescription isodose line (see Equation 4 for the computation of R_{eff}). The gradient score index was used to quantify dose fall-off of the prescription isodose surface to one-half of its value in normal tissue.

$$R_{eff} = \sqrt[3]{\frac{3V}{4\pi}} \qquad (4)$$

Tumour control probability (TCP), the probability of tumour response when the target is irradiated at a given dose for a particular fractionation schedule, was calculated mathematically as:

$$TCP = \left[1 + \left(\frac{TCD_{50}}{gEUD}\right)^{4\gamma_{50}}\right]^{-1} \qquad (5)$$

where TCD_{50} is the dose that gives a response probability of 50% when the tumour is heterogeneously irradiated. γ_{50} is a unitless model parameter that is specific to the normal structure or tumour of interest and describes the slope of the dose–response curve. gEUD is the generalised equivalent uniform dose [12] based on the formalism defined below:

Table 1. Target dose–volume parameters as a function of tumour volume magnitude and multileaf collimator margin

PTV category	Margin (mm)	Minimum dose (Gy)	Maximum dose (Gy)	Mean dose (Gy)
Overall	−1	21.15 ± 1.18 (21.31)	45.82 ± 5.20 (46.29)	34.84 ± 2.38 (34.73)
(n=118)	0	22.07 ± 0.81 (22.22)	35.75 ± 2.11 (35.92)	30.28 ± 1.07 (30.23)
	1	22.93 ± 0.54 (23.01)	30.21 ± 0.89 (30.16)	27.48 ± 0.59 (27.40)
	2	23.51 ± 0.45 (23.55)	27.49 ± 0.62 (27.44)	25.92 ± 0.33 (25.89)
	3	23.78 ± 0.33 (23.80)	26.42 ± 0.54 (26.35)	25.35 ± 0.42 (25.29)
Small	−1	21.30 ± 1.20 (21.51)	46.99 ± 6.00 (47.82)	34.80 ± 2.84 (34.61)
(n=65)	0	22.15 ± 0.85 (22.30)	36.48 ± 2.24 (36.61)	30.36 ± 1.20 (30.35)
	1	23.01 ± 0.43 (23.11)	30.36 ± 0.89 (30.33)	27.44 ± 0.53 (27.40)
	2	23.56 ± 0.27 (23.60)	27.32 ± 0.49 (27.34)	25.81 ± 0.30 (25.80)
	3	23.82 ± 0.16 (23.85)	26.16 ± 0.35 (26.15)	25.16 ± 0.20 (25.14)
Medium	−1	20.94 ± 1.16 (21.19)	45.60 ± 2.81 (46.14)	35.30 ± 1.51 (35.38)
(n=41)	0	21.96 ± 0.76 (22.10)	35.32 ± 1.29 (35.10)	30.34 ± 0.83 (30.24)
	1	22.89 ± 0.66 (22.99)	30.18 ± 0.85 (29.93)	27.58 ± 0.69 (27.41)
	2	23.52 ± 0.65 (23.49)	27.68 ± 0.76 (27.51)	26.01 ± 0.33 (25.93)
	3	23.79 ± 0.50 (23.76)	26.65 ± 0.59 (26.48)	25.54 ± 0.54 (25.38)
Large	−1	21.04 ± 1.04 (21.32)	40.23 ± 2.62 (40.35)	33.52 ± 1.57 (33.04)
(n=12)	0	21.97 ± 0.79 (22.14)	33.28 ± 1.33 (33.24)	29.62 ± 0.91 (29.38)
	1	22.68 ± 0.54 (22.88)	29.52 ± 0.68 (29.43)	27.31 ± 0.50 (27.27)
	2	23.27 ± 0.39 (23.36)	27.77 ± 0.41 (27.87)	26.16 ± 0.33 (26.19)
	3	23.53 ± 0.22 (23.59)	27.04 ± 0.40 (27.22)	25.73 ± 0.23 (25.81)

PTV, planning target volume.
Values presented as mean ± standard deviation, with median values in parentheses.

$$gEUD = \left[\sum_{i=1} v_i \cdot D_i^a \right]^{\frac{1}{a}} \quad (6)$$

where a is a structure-specific unitless volume effect parameter that is negative for tumours and positive for organs-at-risk, and v_i is unitless and represents the ith partial volume receiving dose D_i in Gy. For the purpose of this study, the radiobiological parameters $TCD_{50} = 21.0$ Gy and $\gamma_{50} = 1.25$ [13] and $a = -5$ [14] were used to compute the TCP.

Normal tissue complication probability (NTCP), the probability that a percentage of the patient population will develop an unfavourable reaction for a particular tissue at a given dose for a particular fractionation schedule, was calculated as:

$$NTCP = \left[1 + \left(\frac{TD_{50}}{gEUD} \right)^{4\gamma_{50}} \right]^{-1} \quad (7)$$

where TD_{50} is the tolerance dose for a 50% complication rate at a specific time interval (*e.g.* 5 years in the Emami et al [15] normal tissue tolerance data) when the whole organ of interest is homogeneously irradiated, and γ_{50} is the maximum normalised dose–response gradient. For the purpose of this study, the radiobiological parameters $TD_{50} = 25$ Gy [16], $\gamma_{50} = 3$ [17–18], and $a = 10$ [19–21] were used to compute the NTCP.

It should be emphasised here that the TCP and NTCP analyses in the current study were used as adjuncts to dose-based criteria solely as rankings or comparative tools, and that their absolute values have to be interpreted with caution when making clinical judgments. Finally, the efficiency of each treatment plan was computed as a ratio of the cumulative plan monitor units (MUs) and its corresponding PD.

Statistical analysis

Statistical analyses were performed using PASW Statistics v. 18 (SPSS Inc., Chicago, IL) and SAS v. 9.2 (SAS Institute Inc., Cary, NC). Mixed-model analysis for repeated measures was used to evaluate changes of indices and variables for the five levels of margins. Logarithmic transformation was applied whenever appropriate to address deviation from normality. "Adjust = simulate" option was used to ensure family-wise Type I error rate for multiple testing in comparing group means for SAS LSMEANS procedure. All hypothesis testing was conducted at 5% significance level.

Results

Target volume

Target volumes ranged from 0.03 to 19.54 cm³ (mean/median of 2.17/0.93 cm³), with mean/median of 0.45/0.44 cm³, 2.69/2.62 cm³ and 9.71/8.54 cm³ for small, medium and large PTVs, respectively. The total number of arc degrees per treatment ranged from 510 to 1100 (mean/median of 682/655). Unlike the minimum target dose, which increased with an increase in MLC margin ($p < 0.001$), both mean and maximum target doses decreased with synchronous increasing MLC margin ($p < 0.001$; Table 1 and Figure 1). No predictable pattern was exhibited by each of the target dose–volume parameters and planning target volume. Target dose heterogeneity decreased with increasing MLC margin ($p < 0.001$; Table 2); mean heterogeneity index decreased from 70.1 ± 12.5 to 10.4 ± 2.2%. Despite the manifestation of a definite qualitative correlation between target dose heterogeneity and planning target volume, dose homogeneity apparently increased with target volume for −1, 0 and 1 mm MLC margins, and remained relatively unchanged for 2 and 3 mm margins (Figure 2). Furthermore, target
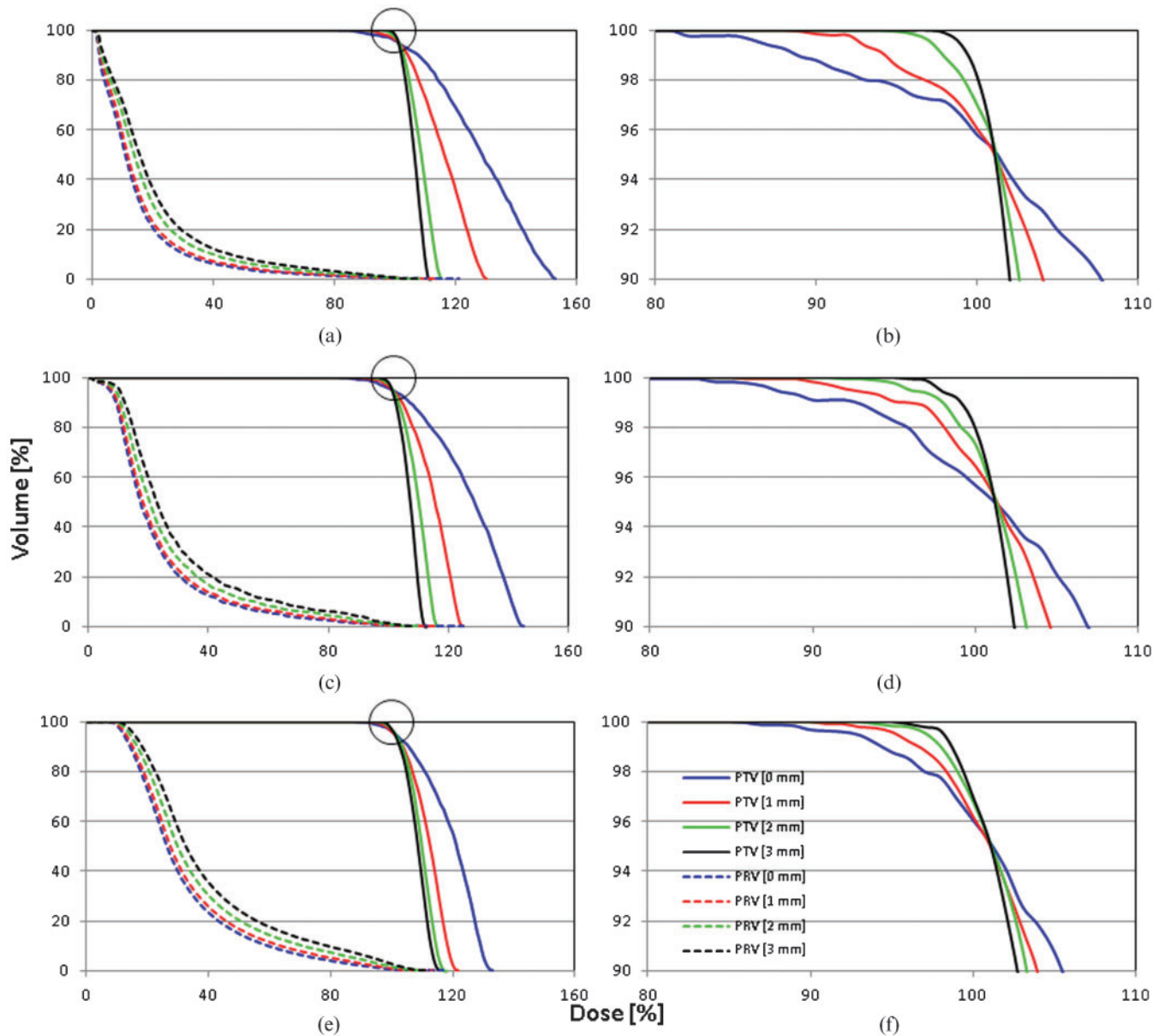
Figure 1. Normal tissue (PRV) and target volume (PTV) dose–volume histograms from representative (a,b) small-sized lesion (0.99 cm³), (c,d) medium-sized lesion (4.88 cm³) and (e,f) large-sized lesion (19.54 cm³). The images on the right are expanded versions of images on the left to emphasise changes in minimum target volume doses as a function of multileaf collimator margin.

dose heterogeneity for small margins (in this case, −1, 0 and 1 mm) were found to be more susceptible to PTV changes than those of large margins (in this case, 2 and 3 mm): ranges included 0.30–1.00 (−1 mm), 0.19–0.67 (0 mm), 0.15–0.41 (1 mm), 0.07–0.24 (2 mm) and 0.04–0.17 (3 mm; see Figure 2). No apparent pattern was observed between target dose conformality and MLC margin (Figure 3). The smallest and largest mean target dose conformality were observed at 1 mm and 3 mm margins, respectively. The mean conformity index ranged from 1.43 ± 0.28 to 1.52 ± 0.23. As expected, target dose conformality improved with planning target volume ($p < 0.001$; Table 2), albeit with poor predictability. Target volume gEUD and its corresponding TCP unequivocally decreased with increasing MLC margin ($p < 0.001$; Table 2); optimal TCP occurred at −1 mm MLC margin (Table 2, Figure 4).

Normal tissue

Normal tissue maximum and mean doses both increased with MLC margin ($p < 0.001$; Table 3) with a general synchronous increase with planning target volume. Normal tissue dose fall-off or gradient increased with MLC margin ($p < 0.001$; Table 2) with lucid planning target volume dependence (Figure 5); mean gradient increased from 3.1 ± 0.9 to 5.3 ± 0.7 mm. Normal tissue gEUD and its corresponding NTCP, on the other hand, did not reveal a clear trend. An optimal NTCP was observed at 1 mm MLC margin for normal tissue receiving greater than 50% of the PD (Figure 6), with apparent increase in the volume of normal tissue receiving greater 50% of the prescription dose as a function of MLC margin (Figure 6).

Table 2. Target dose–volume parameters as a function of tumour volume magnitude and multileaf collimator margin

PTV category	Margin (mm)	HI	CI	gEUD$_{a=-5}$ (Gy)	TCP$_{a=-5}$ (%)
Overall	−1	0.70±0.13 (0.72)	1.43±0.28 (1.35)[a]	30.64±0.87 (30.65)	80.97±2.27 (81.13)
(n=118)	0	0.45±0.07 (0.45)	1.38±0.23 (1.31)[b]	28.85±0.61 (28.85)	75.96±1.98 (76.05)
	1	0.26±0.04 (0.26)	1.37±0.24 (1.31)	27.07±0.50 (27.02)	69.73±1.83 (69.56)
	2	0.15±0.02 (0.15)	1.40±0.22 (1.34)	25.85±0.48 (25.78)	64.63±1.89 (64.37)
	3	0.10±0.02 (0.10)	1.52±0.23 (1.47)	25.30±0.41 (25.25)	62.17±1.76 (61.96)
Small	−1	0.73±0.14 (0.76)	1.52±0.30 (1.41)[a,c]	30.57±1.03 (30.66)	80.73±2.73 (81.14)
(n=65)	0	0.47±0.07 (0.47)	1.47±0.24 (1.39)[b,e]	28.86±0.71 (28.87)	75.98±2.31 (76.11)
	1	0.27±0.04 (0.26)	1.45±0.26 (1.37)[f]	27.03±0.41 (27.01)	69.56±1.60 (69.55)
	2	0.15±0.02 (0.15)	1.47±0.24 (1.41)	25.69±0.26 (25.68)	63.99±1.16 (63.96)
	3	0.09±0.02 (0.09)	1.60±0.23 (1.55)	25.12±0.19 (25.10)	61.36±0.89 (61.29)
Medium	−1	0.70±0.07 (0.71)	1.35±0.22 (1.28)[a]	30.86±0.62 (30.85)	81.58±1.47 (81.60)
(n=41)	0	0.44±0.05 (0.44)	1.28±0.18 (1.23)[b]	28.92±0.45 (28.89)	76.21±1.36 (76.16)
	1	0.26±0.03 (0.25)	1.28±0.18 (1.25)	27.18±0.62 (27.03)	70.12±2.21 (69.62)
	2	0.16±0.02 (0.16)	1.33±0.19 (1.27)	26.02±0.68 (25.84)	65.34±2.53 (64.68)
	3	0.11±0.02 (0.11)	1.44±0.21 (1.38)	25.48±0.54 (25.32)	62.98±2.24 (62.32)
Large	−1	0.57±0.08 (0.57)	1.25±0.19 (1.19)[a,d]	30.33±0.45 (30.20)	80.27±1.16 (79.96)
(n=12)	0	0.38±0.06 (0.38)	1.20±0.10 (1.18)[b]	28.55±0.50 (28.40)	75.03±1.62 (74.57)
	1	0.25±0.04 (0.24)	1.21±0.09 (1.20)	26.96±0.38 (26.97)	69.32±1.48 (69.36)
	2	0.17±0.02 (0.17)	1.28±0.10 (1.30)	26.07±0.28 (26.11)	65.66±1.20 (65.84)
	3	0.14±0.02 (0.14)	1.40±0.13 (1.42)	25.65±0.21 (25.72)	63.78±0.94 (64.14)

a, structure-specific unitless volume effect parameter; CI, conformity index; gEUD, generalised equivalent uniform dose; HI, heterogeneity index; PTV, planning target volume; TCP, tumour control probability.
Values presented as mean ± standard deviation, with median values in parentheses.
$p > 0.01$ [[a](−1 *vs* 2 mm); [b](0 *vs* 1 mm); [c](−1 *vs* 0 mm); [d](−1 *vs* 1 mm); [e](0 *vs* 2 mm); [f](1 *vs* 2 mm)].

Treatment delivery efficiency

The mean monitor unit per centigray of the prescription dose ranged between $1.56 \pm 0.13 \, \text{MU cGy}^{-1}$ and $3.60 \pm 1.30 \, \text{MU cGy}^{-1}$ (Table 4), generally decreasing with MLC margin ($p < 0.001$) and PTV.

Discussion

Because radiosurgery is characteristic of tightly constructed escalated dose schemes that target distinct tumour nodules, the interplay between radiation dose and tumoricidal effect may be assessed without many of the potential concerns that arise when examining tumour cell repopulation during conventional radiotherapy. Furthermore, radiosurgery utilises a higher order of

magnitude of beam trajectories than conventional radiotherapy, to optimise the geometric placement of a radiosurgery dose pattern in order to achieve better target dose conformality and rapid normal tissue dose fall-off. Another key distinction between radiosurgery and conventional radiotherapy is the margin used around the PTV. The principles of choosing an adequate beam margin for conventional radiation therapy are different from those of radiosurgery, in part because of the pre-eminence of dose uniformity within the target volume in conventional radiotherapy. The current study sought to evaluate the consequence of supplemental margins around PTVs on both treatment plan quality metrics and dose–response relationships for the DCA technique involving small fields typical of radiosurgery.
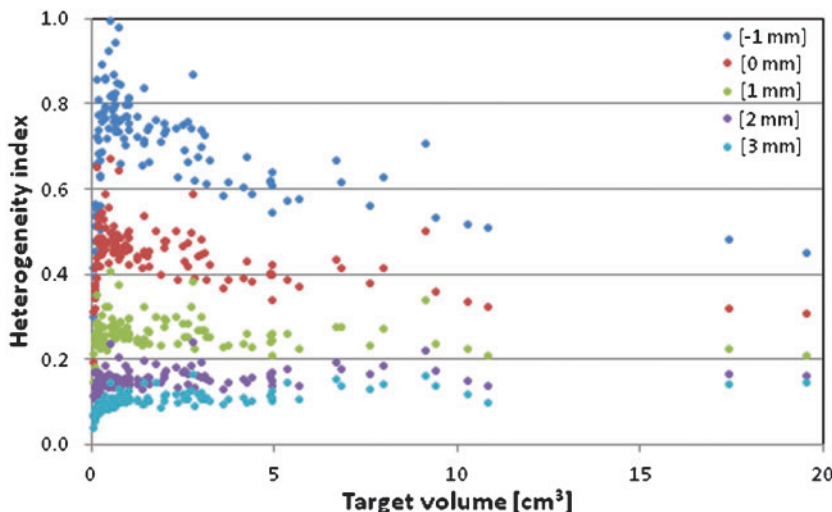

Figure 2. Heterogeneity index distribution as a function of target volume (PTV) for each evaluated multileaf collimator margin.
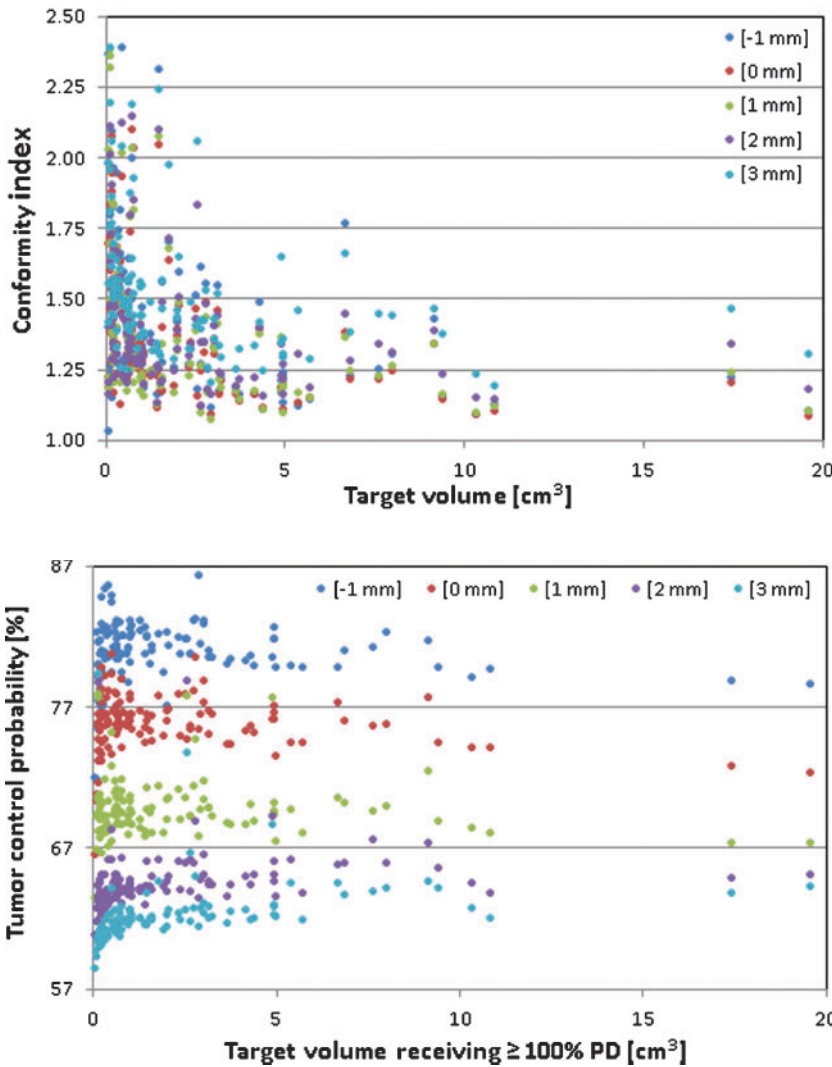
Figure 3. Conformity index distribution as a function of target volume (PTV) for each evaluated multileaf collimator margin.

Figure 4. Tumour control probability distribution as a function of target volume (PTV) receiving doses greater than or equal to the prescription dose for −1, 0, 1, 2 and 3 mm multileaf collimator margins.

Table 3. Normal tissue dose–volume parameters as a function of tumour volume magnitude and multileaf collimator margin

PTV category	Margin (mm)	Maximum dose (Gy)	Mean dose (Gy)	Gradient (mm)	gEUD$_{a=10}$ (Gy)	NTCP$_{a=10}$ (%)
Overall	−1	13.01±4.18 (12.84)	3.64±1.48 (3.35)	3.11±0.94 (2.98)	15.83±1.62 (15.85)[a]	0.74±0.97 (0.42)[a]
(n=118)	0	13.31±3.91 (13.16)	3.68±1.40 (3.41)	3.30±0.86 (3.10)	15.13±1.19 (15.14)[b]	0.35±0.35 (0.24)[b]
	1	14.73±3.88 (14.71)	4.00±1.42 (3.74)	3.81±0.82 (3.71)	15.06±1.10 (14.94)	0.32±0.30 (0.21)
	2	16.92±3.66 (17.08)	4.57±1.47 (4.35)	4.55±0.79 (4.43)	15.47±1.13 (15.41)	0.44±0.42 (0.30)
	3	19.02±3.14 (19.30)	5.25±1.52 (4.98)	5.25±0.69 (5.11)	16.05±1.10 (15.99)	0.65±0.57 (0.47)
Small	−1	10.04±2.58 (10.37)	2.57±0.68 (2.70)	2.47±0.42 (2.45)	15.10±1.51 (15.16)[a,c]	0.40±0.43 (0.25)[a]
(n=65)	0	10.47±2.43 (10.77)	2.66±0.63 (2.71)	2.69±0.33 (2.62)	14.48±1.00 (14.67)[b]	0.19±0.18 (0.17)[d]
	1	11.98±2.51 (12.53)	2.99±0.64 (3.08)	3.26±0.37 (3.30)	14.34±0.73 (14.50)	0.15±0.09 (0.14)
	2	14.36±2.56 (14.70)	3.52±0.68 (3.51)	4.04±0.33 (4.05)	14.69±0.68 (14.82)	0.19±0.10 (0.19)
	3	16.82±2.34 (17.46)	4.15±0.71 (4.26)	4.77±0.29 (4.83)	15.26±0.63 (15.33)	0.30±0.14 (0.28)
Medium	−1	15.80±2.03 (15.97)[e]	4.50±0.74 (4.60)	3.60±0.55 (3.65)	16.63±1.24 (16.48)[a,c]	1.08±1.20 (0.67)[a,c]
(n=41)	0	15.99±1.71 (16.00)	4.50±0.66 (4.50)	3.77±0.41 (3.77)	15.72±0.85 (15.50)[b]	0.46±0.33 (0.32)[b]
	1	17.35±1.96 (18.04)	4.82±0.75 (4.91)	4.23±0.46 (4.18)	15.73±0.71 (15.75)	0.44±0.26 (0.39)
	2	19.45±1.80 (20.03)	5.42±0.78 (5.49)	4.93±0.48 (4.88)	16.17±0.68 (16.25)	0.60±0.39 (0.56)
	3	21.27±1.28 (21.43)	6.16±0.76 (6.18)	5.65±0.39 (5.59)	16.75±0.57 (16.75)	0.88±0.43 (0.81)
Large	−1	19.56±2.01 (18.97)[e]	6.43±0.70 (6.48)	4.90±0.57 (4.85)	17.09±1.35 (16.46)[a,c]	1.48±1.43 (0.66)[a,c]
(n=12)	0	19.51±1.10 (19.29)	6.37±0.63 (6.41)	5.01±0.56 (4.92)	16.56±0.81 (16.27)[b]	1.82±0.51 (0.58)[b]
	1	20.65±0.90 (20.52)	6.71±0.65 (6.70)	5.43±0.56 (5.34)	16.71±0.57 (16.68)	0.85±0.37 (0.77)
	2	22.17±0.64 (22.18)	7.36±0.66 (7.31)	6.00±0.55 (5.93)	17.29±0.44 (17.22)	1.23±0.40 (1.13)
	3	23.24±0.52 (23.26)	8.11±0.70 (8.10)	6.53±0.53 (6.44)	17.88±0.42 (17.89)	1.82±0.56 (1.77)

a, structure-specific unitless volume effect parameter; CI, conformity index; gEUD, generalised equivalent uniform dose; HI, heterogeneity index; PTV, planning target volume; TCP, tumour control probability.
Values presented as mean ± standard deviation, with median values in parentheses.
$p>0.01$ [[a](−1 vs 3 mm); [b](0 vs 1 mm); [c](−1 vs 2 mm); [d](0 vs 2 mm); [e](−1 vs 0 mm)].

Table 4. Number of monitor units necessary to deliver one centigray of prescribed dose as a function of tumour volume magnitude and multileaf collimator margin

Margin (mm)	MU/cGy			
	PTV>0 cm^3 (n=118)	PTV<1 cm^3 (n=65)	1≤PTV<5 cm^3 (n=41)	PTV≥5 cm^3 (n=12)
−1	3.64±1.32 (3.28)	4.35±1.34 (3.88)	2.86±0.41 (2.87)	2.27±0.21 (2.27)
0	2.36±0.43 (2.30)	2.60±0.41 (2.56)	2.11±0.18 (2.06)	1.86±0.16 (1.87)
1	1.86±0.20 (1.85)	1.96±0.19 (1.97)	1.76±0.12 (1.74)	1.63±0.11 (1.62)
2	1.64±0.15 (1.62)	1.69±0.16 (1.68)	1.59±0.11 (1.57)	1.51±0.08 (1.51)
3	1.54±0.12 (1.51)	1.57±0.13 (1.54)	1.52±0.10 (1.50)	1.45±0.07 (1.43)

MU, monitor units; PTV, planning target volume.
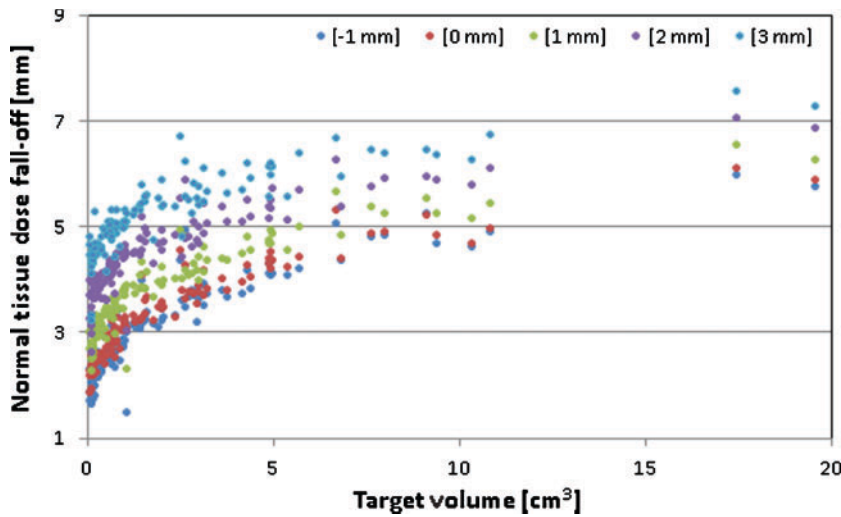Values presented as mean ± standard deviation, with median values in parentheses.

Figure 5. Normal tissue dose fall-off distribution as a function of target volume (PTV) for −1, 0, 1, 2 and 3 mm multileaf collimator margins.

As expected, maximum and mean target doses increased with a synchronous decrease in MLC margin, attributable to the reduction in the number of primary and indirect scatter photons reaching the isocentre, and the ensuing lateral charged particle disequilibrium, with corresponding reduction in field size. In contrast, minimum target dose, like maximum and mean normal tissue doses, increased with increasing MLC margin, since
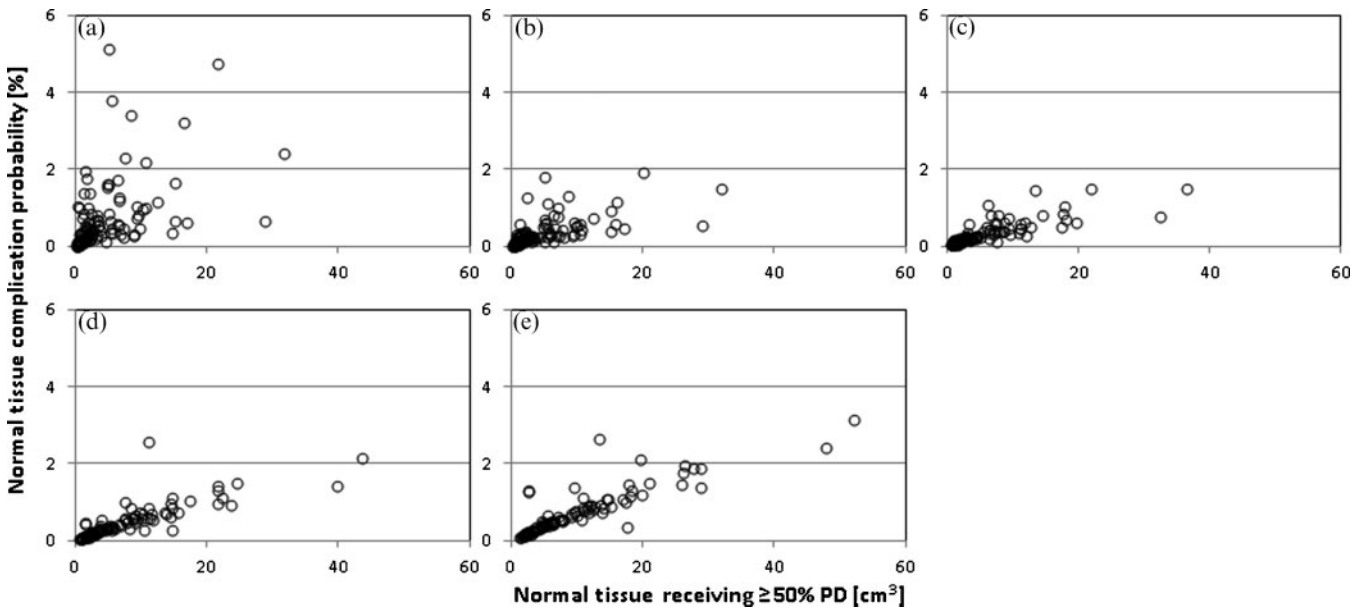

Figure 6. Normal tissue complication probability distribution as a function of target volume (PRV) receiving doses greater than or equal to 50% of the prescription dose. The charts (a) to (e) each represent distributions based on −1, 0, 1, 2 and 3 mm multileaf collimator margins, respectively.

normal tissue dose fall-off increases synchronously with target dose heterogeneity for constant dose normalisation [22]. Findings in the current study also indicate a target volume dependence of dose heterogeneity; specifically, target dose heterogeneity decreasing with PTV for small margins (0 and 1 mm) while remaining relatively constant or increasing slightly for larger margins (2 and 3 mm). In the event when the irradiated volume of tissue is already large (large lesion, in the current study), further increase in MLC margin may not produce a significant difference in normal tissue dose (Table 3 and Figure 3). On the other hand, if the volume of tissue irradiated is small (small lesion, in the current study), an increase in volume due to MLC margin may be acceptable, provided that the increase is not excessive. The critical situation occurs when the normal/critical structure dose approaches its tolerance. In such circumstances, further increase in the volume of (or the dose to) the normal/critical tissue irradiated due to MLC margin may in effect result in a clinically unacceptable situation.

There is the expectation of an optimal MLC margin for simultaneous optimisation of target dose and normal tissue avoidance due to the conflicting contribution of increased dose to normal tissue in the path of the beam for small MLC margins compared with the inclusion of more normal tissue in the beam for large MLC margins. Work by Cardinale et al [6], albeit on lung/liver tumour cases, demonstrated an optimal block margin in the 0 mm range in terms of normal tissue sparing and tumour control [23, 24]. While these results appeared inconsistent with Monte Carlo dose calculation findings by Jin et al [7] for lung cancer stereotactic body radiotherapy, they are in agreement with critical findings in the current study (Tables 1 and 3). An unequivocal optimal value for TCP was observed at smaller margins (specifically, ≤0 mm MLC margin for all cases considered in the current study; Table 2). For NTCP, however, an optimal value was observed at 1 mm MLC margin for most of the cases considered, with up to 24, 42, 5 and 0% of the cases benefiting from −1, 0, 2 and 3 mm MLC margins, respectively (Table 3).

The intent of the present study was not to determine the optimal MLC margin. It should, nonetheless, be emphasised here that it is difficult to arrive at a general mathematical solution to determine the existence of such a margin owing to the interplay of multiple parameters. First, a beam profile is made up of three components: the primary beam, the geometric penumbrae defined by the view of the flattening filter and the dosimetric penumbrae caused by secondary electron spread. In small field regions, the penumbra narrows increasingly as collimator setting is reduced. To understand the source of this change in penumbra width, first consider that the width of an individual geometric penumbra does not change with the position of the collimator, in the same way that a pinhole camera will shift the position of the image if the pinhole is moved without changing its size. However, occlusion of the source causes a drop in the beam output which will affect the part of the penumbra close to the beam axis. This will cause a change in the shape of the high-dose region of the penumbra, which, if the profile is renormalised to 100% on the central axis, results in a narrower penumbra [25]. Finally, observed changes in the total photon energy fluence (*i.e.* the energy from the primary or direct photons and from photons generated in the medium under investigation) with

field size, accelerating potential and depth in water have been shown to be more prominent at potentials below 15 MV [26]. While the corresponding fluence spectra of secondary electrons generated by primary photons alone are independent of field size at field sizes larger than the average electron range (~1.5 cm for the 6 MV photon energy), the total electron fluence distribution varies with field size as a result of electrons originating from scattered photons. As the collimator setting is reduced, the beam output is affected by the lack of lateral electron equilibrium [27] and occlusion of the beam source. Thus, while dose–volume histograms may often look similar, careful analysis of high-dose regions of normal tissues must be performed since significant differences can arise, which may be the most important determinant of control or risk of complication. It is likely that there is an upper limit for the target dose heterogeneity for SRS beyond which the tumour-control probability cannot be improved. If we assume that such a limit exists, the determination of the optimal beam margin must be based on both normal tissue sparing and target dose heterogeneity.

Conclusions

Use of 1 mm MLC margins for dynamic conformal arc-based cranial radiosurgery resulted in optimal tumour control and normal tissue sparing. Clinical significance of these comparative findings warrants further investigation.

Conflicts of interest

JA Tanyi is a speaker for BrainLAB. CD Kubicky is a speaker for BrainLAB. M Fuss is a consultant to and speaker for BrainLAB, Varian Medical Systems and Philips Medical Systems.

Acknowledgments

References

1. Friedman WA. LINAC radiosurgery. Neurosurg Clin N Am 1990;1:991–1008.
2. Hitchcock E, Kitchen G, Dalton E, Pope B. Stereotactic LINAC radiosurgery. Br J Neurosurg 1989;3:305–12.
3. Bortfeld T, Oelfke U, Nill S. What is the optimum leaf width of a multileaf collimator? Med Phys 2000;27:2494–502.
4. Biggs P, Capalucci J, Russell M. Comparison of the penumbra between focused and non-divergent blocks—implications for multileaf collimators. Med Phys 1991;18:753–8.
5. Galvin JM, Han K, Cohen R. A comparison of multileaf collimator and alloy-block field shaping. Int J Radiat Oncol Biol Phys 1998;40:721–31.

6. Cardinale RM, Wu Q, Benedict SH, Kavanagh BD, Bump E, Mohan R. Determining the optimal block margin on the planning target volume for extracranial stereotactic radiotherapy. Int J Radiat Oncol Biol Phys 1999;45:515–20.

7. Jin L, Wang L, Li J, Luo W, Feigenberg SJ, Ma CM. Investigation of optimal beam margins for stereotactic radiotherapy of lung-cancer using Monte Carlo dose calculations. Phys Med Biol 2007;52:3549–61.

8. Grzadziel A, Grosu AL, Kneschaurek P. Three-dimensional conformal versus intensity-modulated radiotherapy dose planning in stereotactic radiotherapy: application of standard quality parameters for plan evaluation. Int J Radiat Oncol Biol Phys 2006;66:S87–94.

9. Paddick I. A simple scoring ratio to index the conformity of radiosurgical treatment plans: technical note. J Neurosurg 2000;93:219–22.

10. Nakamura JL, Verhey LJ, Smith V, Petti PL, Lamborn KR, Larson DA, et al. Dose conformity of gamma knife radiosurgery and risk factors for complications. Int J Radiat Oncol Biol Phys 2001;51:1313–19.

11. Wagner TH, Bova FJ, Friedman WA, Buatti JM, Bouchet LG, Meeks SL. A simple and reliable index for scoring rival stereotactic radiosurgery plans. Int J Radiat Oncol Biol Phys 2003;57:1141–9.

12. Niemierko A. Reporting and analysing dose distributions: a concept of equivalent uniform dose. Med Phys 1997;24:103–10.

13. Mavroidis P, Theodorou K, Lefkopoulos D, Nataf F, Schlienger M, Karlsson B, et al. Prediction of AVM obliteration after stereotactic radiotherapy using radiobiological modelling. Phys Med Biol 2002;47:2471–94.

14. Wu Q, Mohan R, Niemierko A, Schmidt-Ullrich R. Optimization of intensity-modulated radiotherapy plans based on the equivalent uniform dose. Int J Radiat Oncol Biol Phys 2002;52:224–35.

15. Emami B, Lyman J, Brown A, Coia L, Goitein M, Munzenrider JE, et al. Tolerance of normal tissue to therapeutic irradiation. Int J Radiat Oncol Biol Phys 1991;21:109–22.

16. Rubin P. Radiation tolerance of normal tissues. Front Radiat Ther Oncol 1989;23:7–40.

17. Goitein M. The probability of controlling an inhomogeneously irradiated tumor. In: Report of the working group on the evaluation of treatment planning for particle beam radiotherapy. National Cancer Institute, Bethesda, MD; 1987. pp. 1–5.

18. Smith V, Verhey L, Serago CF. Comparison of radiosurgery treatment modalities based on complication and control probabilities. Int J Radiat Oncol Biol Phys 1998;40:507–13.

19. Schultheiss TE, Orton CG, Peck RA. Models in radiotherapy: volume effects. Med Phys 1983;10:410–15.

20. Withers HR, Taylor JM, Maciejewski B. Treatment volume and tissue tolerance. Int J Radiat Oncol Biol Phys 1988;14:751–9.

21. Marks LB, Yorke ED, Jackson A, Ten Haken RK, Constine LS, Eisbruch A, et al. Use of normal tissue complication probability models in the clinic. Int J Radiat Oncol Biol Phys 2010;76:S10–19.

22. Massager N, Maris C, Nissim O, Devriendt D, Salmon I, Levivier M. Experimental analysis of radiation dose distribution in radiosurgery: II. Dose fall-off outside the target volume. Stereotact Funct Neurosurg 2009;87:137–42.

23. Lax I. Target dose versus extra target dose in stereotactic radiosurgery. Acta Oncol 1993;32:453–7.

24. Massager N, Maris C, Nissim O, Devriendt D, Salmon I, Levivier M. Experimental analysis of radiation dose distribution in radiosurgery: I. Dose hot spot inside target volume. Stereotact Funct Neurosur 2009;87:82–7.

25. Das IJ, Ding GX, Ahnesjö A. Small fields: nonequilibrium radiation dosimetry. Med Phys 2008;35:206–15.

26. Yin Z, Hugtenburg RP, Beddoe AH. Response corrections for solid-state detectors in megavoltage photon dosimetry. Phys Med Biol 2004;49:3691–702.

27. Li XA, Soubra M, Szanto J, Gerig LH. Lateral electron equilibrium and electron contamination in measurements of head-scatter factors using miniphantoms and brass caps. Med Phys 1995;22:1167–70.